
Bridging the Knowledge-Prediction Gap in LLMs on Multiple-Choice Questions

Yoonah Park^{*1} Haesung Pyun^{*1} Yohan Jo¹

Abstract

While large language models (LLMs) perform strongly on diverse tasks, their trustworthiness is limited by erratic behavior that is unfaithful to their internal knowledge. In particular, LLMs often fail on multiple-choice questions (MCQs) even if they encode correct answers in their hidden representations, revealing a misalignment between internal knowledge and output behavior. We investigate and mitigate this *knowledge-prediction gap* on MCQs through a three-step analysis of hidden representations. First, we quantify the prevalence and magnitude of the gap across models and datasets. Second, we provide a geometric interpretation by identifying distinct *knowledge* and *prediction* subspaces in the residual stream. Third, we introduce **KAPPA**, a lightweight inference-time intervention that aligns the two subspaces within the residual stream to reduce the knowledge-prediction gap. Our results provide a geometric and interpretable explanation of the knowledge-prediction gap in LLMs. Furthermore, KAPPA effectively reduces the gap across diverse MCQ benchmarks and models, and generalizes to free-form settings.¹

1. Introduction

While large language models (LLMs) exhibit remarkable performance across diverse tasks (Brown et al., 2020; Wei et al., 2022; Kojima et al., 2022), they often make unexpected errors such as hallucinations, systematic biases, and reasoning failures, raising concerns about their trustworthiness (Parrish et al., 2022; Shen et al., 2023; Bang, 2023; Ji et al., 2023; Dziri et al., 2023). In particular, on multiple-choice question (MCQ) benchmarks, a widely used paradigm for evaluating LLMs, models frequently fail to reliably predict correct answers despite possessing the required knowledge. For example, a model may generate a

correct answer in a free-form setting yet select an incorrect option when the same question is presented in an MCQ format (Figure 1a). Prior work has attributed such discrepancies to factors including option selection biases, superficial cues, or stylistic artifacts (Zheng et al., 2024; Balepur et al., 2025; Góral et al., 2025). However, a unified explanation that connects these failures to the model’s internal representations remains unexplored.

Recent studies show that even when models answer incorrectly, their internal representations often linearly encode the correct answer (Liu et al., 2023a; Orgad et al., 2025; Gekhman et al., 2025). A simple linear classifier applied to the hidden states of an LLM frequently predicts the correct answer, even outperforming the model’s own generation. This indicates that models fail to utilize knowledge they already possess—even when such knowledge is explicitly reflected in their hidden states and accessible via simple linear operations. We term this phenomenon *the knowledge-prediction gap*: the discrepancy between the knowledge encoded in a model’s internal representations and the predictions it ultimately generates.

Prior work has identified this gap primarily in limited settings such as truthfulness detection and simple arithmetic tasks (Marks & Tegmark, 2024; Azaria & Mitchell, 2023; Sun et al., 2025a), leaving several questions open: (i) whether this gap extends to diverse domains of MCQ tasks; (ii) what geometric and interpretable structure the model’s hidden representations have; and (iii) whether the gap can be mitigated at inference time without additional training. In this work, we address these questions by (i) establishing that the knowledge-prediction gap is widespread across MCQ benchmarks and the model families, (ii) providing a geometric interpretation of this gap, and (iii) introducing an inference-time intervention that effectively mitigates this gap. We describe these contributions in turn below.

First, we establish that the knowledge-prediction gap is widespread across MCQ benchmarks and the model families. We train a knowledge probe—a linear k -class classifier that predicts the correct answer from the model’s residual stream during question answering (Figure 1, Knowledge Probe). Across a diverse set of models and tasks, we quantify the magnitude of this gap using two complementary metrics and find that it varies substantially across datasets, with some

¹Graduate School of Data Science, Seoul National University. Correspondence to: Yohan Jo <yohan.jo@snu.ac.kr>.

Preprint. February 5, 2026.

¹We will release our code publicly upon publication.

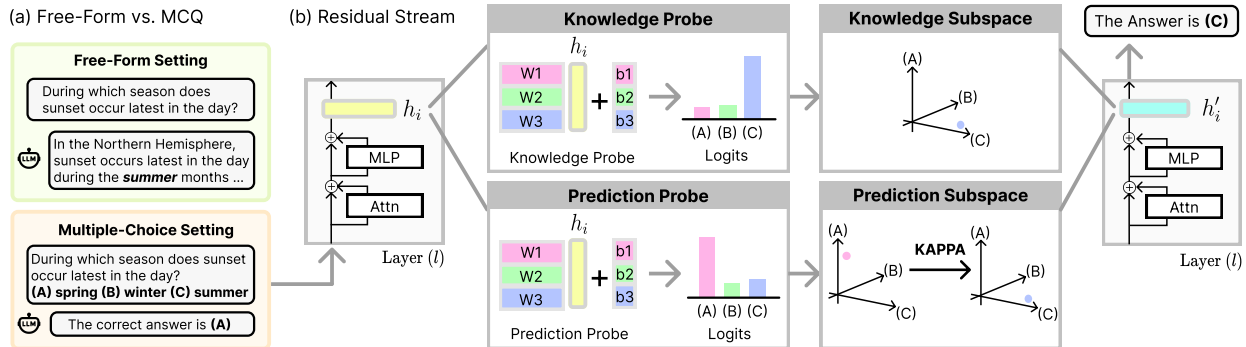


Figure 1. Given a hidden representation h from the residual stream at layer l , we train two linear probes with disjoint objectives: a *knowledge probe* that predicts the ground-truth answer and a *prediction probe* that predicts the option decoded by the LLM. Although both probes operate on the same hidden state, their logits and the resulting coordinate representations differ. Interpreting probe weight vectors as defining low-dimensional subspaces, this discrepancy shows a misalignment between the coordinates of h in the knowledge subspace and the prediction subspace.

benchmarks exhibiting particularly pronounced gaps.

Second, we provide a geometric interpretation of the gap. The knowledge probe produces a distribution over k answer choices, and these logits can be viewed as coordinates in a k -dimensional subspace of the model’s representation space (which we call *knowledge subspace*; later discussed). We train an analogous prediction probe that predicts the model’s generated answer choice, defining a corresponding *prediction subspace* (Figure 1, Prediction Subspace). Ideally, the coordinates in the prediction subspace—indicating which option the model chooses—should align with the coordinates in the knowledge subspace—indicating which option is likely to be correct. However, we find that when the knowledge-prediction gap is large, the two subspaces exhibit systematic misalignment, providing a geometric explanation of the gap.

Third, we introduce an inference-time intervention to mitigate the gap. Our method, KAPPA (**K**nowledge-**A**ligned **P**rediction through **P**rojection-based **A**ddjustment), applies an affine transformation to the model’s residual stream that aligns the prediction subspace with the knowledge subspace while minimally perturbing the original representation (Figure 1, KAPPA). Unlike prior steering methods that apply a fixed correction uniformly across all inputs, KAPPA adapts its adjustment to each instance based on its own knowledge-prediction gap.

We find that the knowledge-prediction gap is a widespread phenomenon in large language models, persisting across five representative models and a diverse set of MCQ benchmarks spanning reasoning, knowledge, truthfulness, and bias. The gap is most pronounced on reasoning, truthfulness, and bias benchmarks, while being substantially less evident on knowledge-intensive benchmarks. Moreover, this gap remains consistent across model families and scales for certain tasks, suggesting that it reflects a structural limitation

rather than a model-specific artifact.

Our intervention, KAPPA, consistently reduces this gap and improves accuracy over existing inference-time approaches. These results suggest that many LLM failures stem not from missing knowledge, but from a misalignment between what the model internally encodes and what it ultimately predicts. Further analysis reveals that the identified knowledge and prediction subspaces partially transfer across tasks requiring similar skills, and even to free-form generation settings. Overall, our findings highlight representation-level alignment as a promising direction for eliciting more faithful predictions from LLMs.

Our contributions are threefold:

- We empirically reveal a **knowledge-prediction gap** in general MCQs by introducing quantitative metrics.
- We reveal the geometric structure underlying the gap: a misalignment between knowledge and prediction subspaces in the residual stream.
- We present KAPPA, an inference-time intervention that geometrically calibrates hidden states to align model predictions with the internal knowledge.

2. Related Work

The Knowledge-Prediction Gap. Prior work shows that linear probes can extract correct answers from hidden representations even when the model outputs are incorrect (Marks & Tegmark, 2024; Liu et al., 2023a; Azaria & Mitchell, 2023; Wang et al., 2024; Su et al., 2024; Orgad et al., 2025; Gekhman et al., 2025). Several explanations have been proposed, including distractor-driven mechanisms that override correct knowledge (Tulchinskii et al., 2024; Wiegrefe et al., 2025; Yang et al., 2025) and miscalibration between early knowledge-encoding layers and later prediction-generating

layers (Gottesman & Geva, 2024). However, most prior work examines this phenomenon in constrained settings such as truthfulness or arithmetic tasks (Liu et al., 2023a; Sun et al., 2025a), and focuses primarily on identifying the gap rather than closing it.

Inference-Time Intervention. Recent work has explored modifying model behavior through representation-level interventions (Zou et al., 2025; Arditi et al., 2024; Rimsky et al., 2024; Hendel et al., 2023; Ilharco et al., 2023). Inference-time intervention methods typically train linear probes to identify meaningful directions in hidden representations and then steer model activations accordingly (Li et al., 2023; von Rütte et al., 2024). These techniques have been applied to objectives such as toxicity mitigation (Turner et al., 2023; Liu et al., 2023b), safety (Zou et al., 2023; Rimsky et al., 2024; Lee et al., 2025), and reasoning (Venhoff et al., 2025). Decoding-based approaches have also been proposed; for example, Chuang et al. (2024) contrast layer-wise logits to amplify factual signals. However, these methods have not been systematically evaluated for reducing the knowledge-prediction gap.

In this paper, we bridge these two lines of research: we provide a geometric interpretation of the knowledge-prediction gap and introduce KAPPA, an inference-time intervention that aligns the prediction subspace with the knowledge subspace by modifying internal representations. We later show that KAPPA consistently outperforms existing approaches in reducing the gap.

3. The Knowledge-Prediction Gap in MCQs

In this section, we demonstrate the **knowledge-prediction gap** in MCQ settings. We first use linear probing to identify knowledge- and prediction-related signals in the model’s hidden states, quantify the gap, and finally analyze the representation geometry to explain its emergence.

We define the **knowledge-prediction gap** as the discrepancy between the knowledge encoded in a model’s internal representations and the predictions it ultimately generates. Whether a model “possesses” certain knowledge can be assessed in various ways, depending on the form in which that knowledge is encoded. In this work, we focus on cases where the model possesses knowledge in a **linearly accessible** form—knowledge that can be extracted through simple linear operations on hidden states. For a MCQ with k options, we train a linear probe that maps the model’s hidden representation to a k -dimensional vector, where each dimension reflects the likelihood of the corresponding option being correct. When such a probe accurately predicts the correct answer, we consider the model to possess the linearly accessible knowledge. While richer knowledge might be encoded in non-linear forms, we focus on linear accessibility

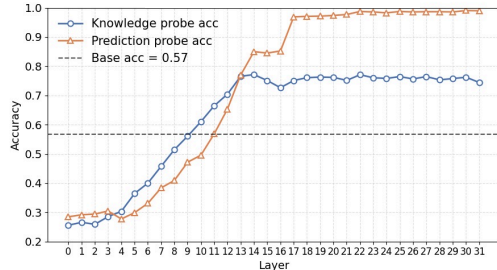


Figure 2. Layer-wise accuracy of the knowledge probe and the prediction probe on TruthfulQA for Llama 3.1 8B Instruct. While the knowledge probe accuracy increases steadily and saturates at higher layers, the prediction probe exhibits a sharper transition, lagging behind in earlier layers. The dashed line indicates the base model accuracy, highlighting a substantial knowledge-prediction gap in intermediate layers.

because it represents the most interpretable and steerable form of knowledge. Furthermore, since this is the easiest form of knowledge to exploit, its common underutilization makes it implausible that the model effectively leverages more complex forms of knowledge.

3.1. Linear Probing Analysis

In this subsection, we conduct a probing analysis across diverse MCQ benchmarks and two LLM families to examine whether models exhibit a consistent behavior: generating incorrect predictions despite possessing linearly accessible knowledge of the correct answer. Specifically, we train two linear probes on the model’s residual stream activations with distinct objectives: a knowledge probe that predicts the ground-truth answer, and a prediction probe that predicts the answer option ultimately chosen by the LLM.

To train the probes, we extract residual stream activations from each layer of the L layers of the LLM. For each input prompt x containing a multiple-choice question (Figure 1, left), we record the ground-truth label $y \in \{1, \dots, k\}$ and the LLM’s predicted choice $\tilde{y} \in \{1, \dots, k\}$. At every layer l , we extract the activation at the last token position, denoted $h^l(x) \in \mathbb{R}^d$, and construct two datasets: a knowledge dataset $D_{\text{know}}^{(l)} = \{(h^l(x), y)\}$ pairing activations with ground-truth labels, and a prediction dataset $D_{\text{pred}}^{(l)} = \{(h^l(x), \tilde{y})\}$ pairing activations with model predictions. We train two single-layer linear classifiers with k -class softmax outputs: a knowledge probe trained on $D_{\text{know}}^{(l)}$ to predict y , and a prediction probe trained on $D_{\text{pred}}^{(l)}$ to predict \tilde{y} . Both knowledge and prediction probes are trained independently at each layer, yielding L probes of each type. We select the layer with the highest knowledge probe accuracy where prediction accuracy exceeds 85% on the validation set. See Appendix C.3 for details about probe selection.

Table 1. Model- and dataset-wise comparison of the knowledge-prediction gap for Qwen 2.5 7B Instruct and Llama 3.1 8B Instruct. We report task accuracy of the base model (ACC), the relative accuracy gain of the knowledge probe over the base model (Δ ACC), and knowledge-prediction gap metrics (AGR and KLD). Higher values of Δ ACC and AGR indicate smaller knowledge-prediction gaps, and lower KLD indicates closer alignment between encoded knowledge and model predictions. The value k denotes the number of answer options for each MCQ benchmark. Boldface highlights the top three results within each column.

Category	Dataset	k	Qwen 2.5 7B				Llama 3.1 8B			
			ACC	Δ ACC	AGR	KLD	ACC	Δ ACC	AGR	KLD
Reasoning	GSM8k	4	47.8	+2.5	60.3	0.86	32.6	+4.1	53.7	0.35
	BBH-Algorithmic	4	51.0	+4.4	69.6	0.70	45.1	+5.5	62.1	0.23
	BBH-NLP	4	61.1	+5.1	69.8	0.92	59.6	+3.9	73.9	0.41
Knowledge	MMLU Humanities	4	59.9	+2.6	78.5	0.78	58.6	+3.4	77.9	0.47
	MMLU Social Sciences	4	78.8	+0.2	95.9	0.72	74.0	-0.6	90.5	0.47
	MMLU STEM	4	65.2	+0.2	89.7	0.70	54.7	+0.2	91.1	0.32
	ARC-Challenge	3	90.9	+0.0	98.5	0.55	85.0	+0.2	98.0	0.43
	PubMedQA	3	72.3	-0.3	89.8	0.57	75.7	+0.0	96.4	0.43
Truthfulness & Bias	TruthfulQA	4	58.8	+21.3	61.8	1.01	56.7	+19.6	62.1	0.63
	BBQ-Age	3	83.2	+9.3	84.0	0.68	59.9	+29.3	59.2	0.59
	BBQ-Religion	3	79.6	+0.7	98.5	0.54	67.6	+10.6	79.1	0.42

Setup We use LLaMA 3.1 8B Instruct and Qwen2.5 7B Instruct as representative open-weight models. Evaluation is conducted on a diverse suite of multiple-choice benchmarks including BBH (algorithmic and linguistic subtasks) (Suzgun et al., 2023), MMLU (STEM, Humanities, and Social Sciences) (Hendrycks et al., 2021), ARC-Challenge (Clark et al., 2018), TruthfulQA (Mahaut et al., 2024), GSM8K (Cobbe et al., 2021), PubMedQA (Jin et al., 2019), and BBQ (Age and Religion) (Parrish et al., 2022). A complete list of subtasks and dataset statistics is provided in Appendix A.

Quantitative Metrics Since the accuracy (ACC) alone does not quantify magnitude of the knowledge-prediction gap in a way that allows comparison across benchmarks and models, we introduce two complementary metrics. Let $p_K \in \Delta^k$ denote the option distribution induced by the *knowledge probe*, and let $p_M \in \Delta^k$ denote the distribution generated by the model, where Δ^k is the k -dimensional probability simplex. Both distributions are obtained by applying a softmax over option-level logits.

(1) Prediction Agreement We measure decision-level alignment by checking whether the two distributions select the same option:

$$\text{AGR}(x) = \mathbb{I}\left[\arg \max_i p_K(i) = \arg \max_i p_M(i)\right]. \quad (1)$$

Higher AGR indicates that the model’s predictions more often match its encoded knowledge.

(2) Distributional Divergence Decision agreement does not capture differences in confidence across options. We therefore measure distribution-level alignment using Kullback-Leibler divergence:

$$\text{KLD}(x) = \text{KL}(p_M \parallel p_K). \quad (2)$$

Lower KLD indicates closer alignment between the model’s output distribution and its encoded knowledge. Note that KLD is comparable only across benchmarks with the same number of options k .

Results Table 1 shows the performance of the selected knowledge probes on each test set. The knowledge probes consistently outperform the LLMs’ generation accuracy, with positive accuracy gains (Δ ACC) observed across both model families and benchmarks. The layer-wise analysis (Figure 2, Appendix 7) reveals that this advantage emerges after the middle layers, where knowledge probe accuracy increases sharply—reaching up to 92.5% point on certain datasets. These results confirm that models encode linearly accessible knowledge that they fail to use in their final generations. Prediction probes achieve even higher accuracy than knowledge probes, often exceeding 90% point, indicating that the model’s eventual output is also strongly represented in hidden states. Together, these findings establish that hidden states robustly encode both the correct answer and the model’s generated answer—yet these two signals diverge.

The magnitude of the knowledge-prediction gap varies substantially across benchmark domains. Across two representative open-weight models, the gap is substantially larger for **truthfulness & bias** and **reasoning** benchmarks, whereas it remains comparatively small for **knowledge** benchmarks. For truthfulness & bias tasks, we hypothesize that models override their encoded knowledge with a preference for hasty answering—providing definite answers even when abstention is appropriate (Yang et al., 2024; Wen et al., 2024). For example, on BBQ, where many questions require selecting “undetermined”, Qwen2.5 7B Instruct chooses this option in only 13–27% of cases (accuracy: 56.7–59.9% point), while knowledge probes achieve 38–51% (accuracy: 76.3–89.2% point). Hence, mitigating the knowledge-

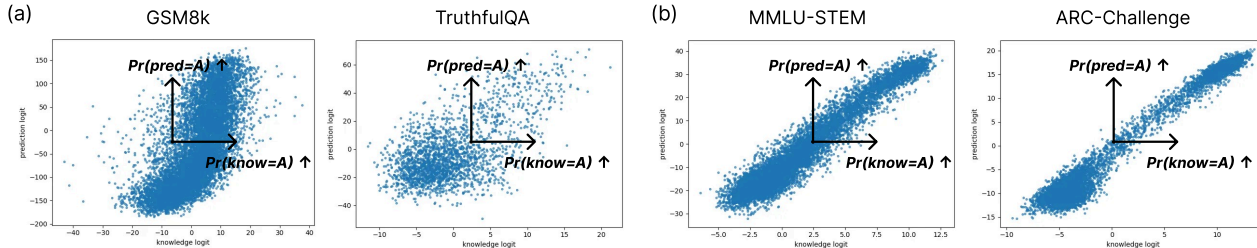


Figure 3. Scatter plots of hidden-state activations from Qwen2.5 7B Instruct, where each point corresponds to a pair of logits: the *knowledge logit* and the *prediction logit* for the first answer option. Results are shown for GSM8K (27th layer), TruthfulQA (19th layer), MMLU-STEM (23rd layer), and ARC-Challenge (24th layer). For datasets with a small knowledge-prediction gap (a), the two probe logits are well aligned, whereas datasets exhibiting a larger gap (b) show greater misalignment between knowledge and prediction signals.

prediction gap may help reduce hallucinations. For reasoning tasks, we hypothesize that models trained to generate intermediate traces may not fully leverage their internal representations when producing a final answer directly (Ma et al., 2025; Sun et al., 2025b). Therefore, reducing the gap holds potential for improving reasoning efficiency by requiring fewer tokens. In the following section, we analyze the gap geometrically to better understand its underlying structure.

3.2. Geometric Analysis

To better understand the representation geometry underlying the knowledge-prediction gap, we analyze the model’s residual stream using the knowledge and prediction probes.

Setup We interpret the weights of trained knowledge probes and prediction probes as the axes of each corresponding subspace within the residual stream (Figure 1, top). Given a MCQ with k options, the knowledge probe is parameterized by a weight matrix $W \in \mathbb{R}^{d \times k}$ and a bias vector $b \in \mathbb{R}^k$. The probe produces a k -dimensional logit vector, where the i -th logit is computed as $w_i^\top h$, with h denoting the residual stream activation and w_i the i -th column of W (we omit the bias term for clarity). Each logit can be interpreted as the projection of h onto w_i , where a larger value indicates that the hidden state assigns a higher probability to option i being the correct answer. Building on this, we treat the probe weight vectors $\{w_i\}_{i=1}^k$ as axes spanning a k -dimensional subspace of the residual stream. Under this construction, each activation h is mapped to a point in the subspace, whose coordinates are represented by the probe logits. Formally, each subspace corresponds to the column space of the respective probe weight matrix, yielding the *knowledge subspace* $\text{span}(W_{\text{know}})$ and the *prediction subspace* $\text{span}(W_{\text{pred}})$.

These subspaces provide a geometric lens for analyzing how encoded knowledge and model predictions diverge within the representation space. Ideally, the coordinates of a hidden state projected onto the knowledge and predic-

tion subspaces should be well aligned. However, when a knowledge-prediction gap arises, we observe a systematic misalignment between these two subspaces.

Results Figure 3 illustrates this phenomenon by extracting the k -dimensional logits from the knowledge and prediction probes at inference time and plotting the logits corresponding to the first answer option. The datasets identified with a large knowledge-prediction gap in the previous section, such as GSM8K and TruthfulQA, exhibit substantial off-diagonal misalignment between the two logits (Figure 3a), whereas datasets with a smaller gap, such as MMLU-STEM and ARC-Challenge, show much stronger diagonal alignment (Figure 3b). These results demonstrate that the knowledge-prediction gap is reflected in the geometry of the residual stream, motivating our approach of aligning these subspaces at inference time to mitigate the gap.

4. Bridging the Knowledge-Prediction Gap

To mitigate the knowledge-prediction gap in MCQs, we introduce KAPPA (**K**nowledge-**A**ligned **P**rediction through **P**rojection-based **A**ddjustment), an inference-time intervention that applies affine transformations to the residual stream. Motivated by the observed misalignment between the knowledge and prediction subspaces, KAPPA aligns the model’s prediction with the knowledge encoded in the hidden states through a simple geometric correction.

4.1. Knowledge-Aligned Prediction Adjustment

Given an input prompt x containing a multiple-choice question, KAPPA extracts the residual stream activation $h = h^l(x)$ at a layer l for the last token of the prompt. It then computes the geometric coordinates of h within the knowledge and prediction subspaces, as identified by the two linear probes. KAPPA minimally adjusts the hidden state within the prediction subspace so that its coordinates align with those in the knowledge subspace. This intervention is applied at each decoding step from the last token of the prompt to all subsequently generated tokens.

Table 2. Results across benchmarks for Qwen 2.5 7B Instruct and Llama 3.1 8B Instruct. Higher Δ ACC and AGR indicate smaller knowledge-prediction gaps, while lower KLD reflects closer alignment between encoded knowledge and model predictions. Benchmark names annotated with (\cdot) denote the number of answer options in the corresponding MCQ setting. The KP rows report results computed directly from the knowledge probe’s predictions. For KAPPA (\cdot) , the value in parentheses denotes the number of layers intervened at inference time. Boldface indicates the best result among {Base, CAA, DoLA, KAPPA (\cdot) }, excluding the KP row.

Model	Method	GSM8k (4)			BBH-Algo (4)			BBH-NLP (4)			TruthfulQA (4)			BBQ-Age (3)			BBQ-Religion (3)		
		ACC	AGR	KLD	ACC	AGR	KLD	ACC	AGR	KLD	ACC	AGR	KLD	ACC	AGR	KLD	ACC	AGR	KLD
Qwen 2.5 7B	Base	47.8	60.3	0.86	51.0	69.6	0.70	61.1	69.8	0.92	58.8	61.8	1.01	83.2	84.0	0.68	79.6	98.5	0.54
	CAA	47.7	60.3	0.85	51.2	69.8	0.71	61.2	69.9	0.92	61.1	63.5	0.98	84.3	85.0	0.67	79.5	98.5	0.54
	DoLA	48.1	60.0	0.86	50.4	67.5	0.75	61.0	69.3	0.92	58.5	61.3	1.02	82.9	83.9	0.68	79.5	98.2	0.54
	KAPPA (1)	49.6	68.8	0.78	51.5	72.5	0.69	63.0	74.0	0.89	60.6	64.0	0.99	84.1	85.2	0.67	80.1	99.4	0.55
	KAPPA (3)	49.1	65.4	0.77	52.2	75.3	0.65	62.8	73.2	0.89	61.9	65.1	0.97	83.9	84.9	0.67	80.2	99.0	0.55
	KAPPA (6)	49.2	66.3	0.76	53.6	78.9	0.66	63.6	74.9	0.87	64.1	67.3	0.95	85.5	87.0	0.64	80.5	98.8	0.55
	KP	50.3	100.0	0.00	55.4	100.0	0.00	66.2	100.0	0.00	80.1	100.0	0.00	92.5	100.0	0.00	80.3	100.0	0.00
Llama 3.1 8B	Base	32.6	53.7	0.35	45.1	62.1	0.23	59.6	73.9	0.41	56.7	62.1	0.63	59.9	59.2	0.59	67.6	79.1	0.42
	CAA	32.9	53.8	0.38	45.1	62.1	0.26	60.2	73.3	0.41	62.3	67.2	0.60	65.8	64.8	0.53	68.8	80.0	0.42
	DoLA	33.2	49.7	0.58	42.4	47.4	0.29	56.6	69.6	0.51	55.6	61.6	0.76	59.6	60.1	0.64	64.9	76.6	0.42
	KAPPA (1)	34.9	73.8	0.37	49.3	83.1	0.31	62.4	86.3	0.47	67.8	78.8	0.60	73.8	75.0	0.45	75.7	93.6	0.46
	KAPPA (3)	34.6	66.2	0.27	49.2	81.9	0.26	63.0	83.7	0.39	73.5	77.6	0.48	72.3	74.4	0.38	76.5	92.9	0.41
	KAPPA (6)	36.6	75.9	0.27	50.1	82.5	0.30	60.2	75.3	0.46	65.5	72.9	0.46	76.8	81.1	0.31	68.8	81.6	0.57
	KP	36.6	100.0	0.00	50.7	100.0	0.00	63.5	100.0	0.00	76.3	100.0	0.00	89.1	100.0	0.00	78.1	100.0	0.00

We formalize this intervention as a constrained optimization problem that adjusts hidden states to align prediction coordinates with corresponding knowledge coordinates, while remaining close to the original representations. For a hidden state h , we derive a transformation $\mathcal{T} : \mathbb{R}^d \rightarrow \mathbb{R}^d$ that maps h to a modified state $h' = \mathcal{T}(h)$ under the following constraints: (1) *Alignment constraint*: the modified prediction coordinates must align with the knowledge coordinates; (2) *Minimal Perturbation*: the perturbation $\|h' - h\|$ is minimized so as to preserve other information.

Given the probe weights $W_{\text{pred}}, W_{\text{know}} \in \mathbb{R}^{d \times k}$ and biases $b_{\text{pred}}, b_{\text{know}} \in \mathbb{R}^{k \times 1}$, we derive the hidden-state update by solving the following constrained optimization problem:

$$\min_{\tilde{h}'} \|\tilde{h}' - \tilde{h}\|_2^2 \quad \text{s.t.} \quad \tilde{W}_{\text{pred}}^\top \tilde{h}' = \tilde{W}_{\text{know}}^\top \tilde{h}, \quad (3)$$

where we use augmented notations

$$\tilde{h}' = \begin{bmatrix} h' \\ 1 \end{bmatrix}, \quad \tilde{h} = \begin{bmatrix} h \\ 1 \end{bmatrix},$$

$$\tilde{W}_{\text{know}} = \begin{bmatrix} W_{\text{know}} \\ b_{\text{know}}^\top \end{bmatrix}, \quad \tilde{W}_{\text{pred}} = \begin{bmatrix} W_{\text{pred}} \\ b_{\text{pred}}^\top \end{bmatrix} \in \mathbb{R}^{(d+1) \times k}.$$

Solving Eq. 3 yields a closed-form solution corresponding to the minimal ℓ_2 modification that aligns the prediction coordinates with the knowledge coordinates (full derivation provided in Appendix B):

$$\tilde{h}' = \tilde{h} + \tilde{W}_{\text{pred}} \left(\tilde{W}_{\text{pred}}^\top \tilde{W}_{\text{pred}} \right)^{-1} \left(\tilde{W}_{\text{know}}^\top \tilde{h} - \tilde{W}_{\text{pred}}^\top \tilde{h} \right).$$

This update modifies the hidden state only within the prediction subspace, leaving orthogonal components unchanged, while ensuring geometric alignment with the knowledge subspace. Unlike typical steering methods that apply fixed modifications across all inputs, KAPPA dynamically computes

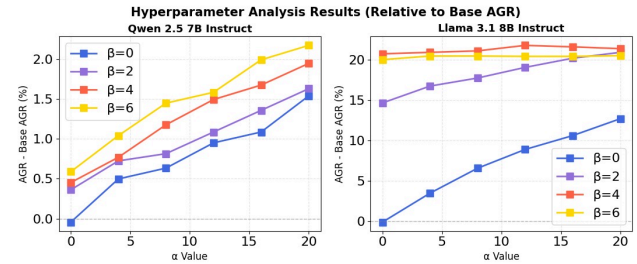


Figure 4. Effect of parameters α and β on agreement rate improvement over the base model. (Left) Qwen2.5 7B Instruct results across six α values and four β values. (Right) Llama 3.1 8B Instruct results under the same settings.

the minimal adjustment required based on the knowledge and prediction coordinates.

Generalized Alignment While the original alignment constraint in Eq. 3 enforces strict equality between the knowledge and prediction coordinates, we extend our method to a more general form to capture more diverse knowledge-prediction relationships. We parameterize the target mapping with hyperparameters $\alpha, \beta \in \mathbb{R}$:

$$\tilde{W}_{\text{pred}}^\top \tilde{h}' = \alpha \cdot \tilde{W}_{\text{know}}^\top \tilde{h} + \beta \cdot \text{sign}(\tilde{W}_{\text{know}}^\top \tilde{h}). \quad (4)$$

The original constraint is recovered when $\alpha = 1$ and $\beta = 0$, while larger values of α and β amplify the influence of internal knowledge on model predictions. The larger offset β introduces a stronger margin that encourages the model to favor the option indicated by the knowledge probe, even when the knowledge signal is weak.

4.2. Experiments

Setup Using the identified knowledge and prediction subspaces for each dataset, we evaluate KAPPA at inference time on six diverse benchmarks showing a large

Table 3. Average accuracy (ACC), agreement (AGR), and KL divergence (KLD) across multiple models on the TruthfulQA benchmark. For KAPPA(\cdot), the value in parentheses denotes the number of layers intervened at inference time. Boldface indicates the best result among {Base, CAA, DoLA, KAPPA(\cdot)}, excluding the knowledge probe (KP).

Method	Mistral v0.3 7B			Llama-3.1 8B			Qwen 2.5 7B			Qwen3 4B			Qwen3 14B		
	ACC	AGR	KLD	ACC	AGR	KLD	ACC	AGR	KLD	ACC	AGR	KLD	ACC	AGR	KLD
Base	40.7	46.6	0.94	56.7	62.1	0.63	58.8	61.8	1.01	56.5	60.0	0.82	71.6	76.0	0.76
CAA	52.8	55.9	0.83	62.3	67.2	0.60	61.1	63.5	0.98	60.1	63.2	0.83	73.6	77.9	0.76
DoLA	40.5	46.7	0.94	55.6	61.6	0.76	58.5	61.3	1.02	56.5	59.4	0.83	71.3	75.9	0.77
KAPPA (1)	51.0	59.7	0.82	67.8	78.8	0.60	60.6	64.0	0.99	58.4	62.3	0.79	73.3	78.1	0.76
KAPPA (3)	56.3	64.1	0.68	73.5	77.6	0.48	61.9	65.1	0.97	58.9	62.6	0.75	74.3	79.2	0.74
KAPPA (6)	58.3	62.3	0.65	65.5	72.9	0.46	64.1	67.3	0.95	61.4	66.1	0.70	77.7	83.7	0.72
KP	69.5	100.0	0.00	76.3	100.0	0.00	80.1	100.0	0.00	78.7	100.0	0.00	85.8	100.0	0.00

knowledge-prediction gap in Section 3.1. Furthermore, to examine whether KAPPA generalizes across model architectures and sizes, we additionally evaluate KAPPA on Mistral 7B Instruct v0.3, Qwen3 4B, and Qwen3 14B using the TruthfulQA dataset. For KAPPA intervention, we select the top- n consecutive layers with the highest knowledge probe accuracies from those where the prediction probe accuracy exceeds a threshold. Details of the evaluation protocol are provided in Appendix C.3.

To compare KAPPA’s effectiveness with prior inference-time methods in reducing the knowledge-prediction gap, we consider the following baselines: (i) **Base**: the original LLM; (ii) **CAA**: activation steering using difference-in-means vectors (Rimsky et al., 2024); (iii) **DoLA**: a decoding method that contrasts layer-wise logits (Chuang et al., 2024). More details are provided in Appendix C.4.

Results Across Datasets Table 2 demonstrates the effectiveness of KAPPA across six diverse benchmarks spanning reasoning, truthfulness, and bias domains, where substantial knowledge-prediction gaps are observed. As shown in the AGR column, KAPPA consistently improves over base models and prior inference-time methods by significantly increasing agreement between the knowledge probe and the model’s final predictions (up to 17.5% points). Crucially, these improved agreements translate into substantial gains in accuracy, often approaching the accuracy of the knowledge probe (KP), which is achieved when the model fully utilizes its linearly accessible knowledge. The gains are especially pronounced in truthfulness and bias benchmarks: for LLaMA 3.1 8B, KAPPA achieves improvements of 8.9–16.9 points on TruthfulQA and BBQ, while delivering consistent gains of 1.5–5.0 points in reasoning benchmarks. Conversely, on knowledge benchmarks where the knowledge-prediction gap is negligible, KAPPA yields only modest changes (see Appendix D.2). This confirms that our method mitigates the misalignment between internal knowledge and output prediction.

Results Across Models Table 3 indicates that the knowledge-prediction gap is a pervasive phenomenon across

a broad range of model families and sizes. Although larger-scale models tend to exhibit a relatively narrower gap compared to smaller counterparts (AGR: 76% for Qwen3 14B vs. 60% for Qwen3 4B), the misalignment remains substantial. KAPPA effectively mitigates this persistent gap across all evaluated models, suggesting that the misalignment is causally mediated by low-dimensional subspaces within the model’s representations regardless of scale. Overall, these results support our hypothesis that many model errors arise from a geometric misalignment between internal knowledge and output predictions.

Hyperparameter Sweep To study the causal roles of the alignment parameters α and β in Eq. 4, we perform a hyperparameter sweep, training and evaluating probes on TruthfulQA. Varying α and β induces clear effects: increasing either parameter improves agreement (Figure 4). This improvement arises because larger values amplify the prediction coordinate, steering model outputs toward the knowledge probe’s selected answer. Overall, these results confirm that α and β causally control the extent to which model predictions reflect linearly encoded knowledge.

5. Analysis

5.1. KAPPA Generalization Across Datasets

To examine whether the identified subspaces generalize across datasets, we conduct a cross-dataset transfer analysis, in which subspaces extracted from one dataset are directly applied to another. Figure 5 reports transfer effects measured by improvements in agreement relative to the base model. Overall, the results show limited transferability, indicating that different datasets and tasks have geometrically distinct knowledge and prediction subspaces.

Nevertheless, we observe successful transfer in some settings. These cases involve transfers within the same category, where the source and target datasets require broadly similar underlying skills. For example, applying subspaces extracted from BBH-NLP to GSM8K yields a 4.81% point gain, and transferring subspaces from TruthfulQA to BBQ-

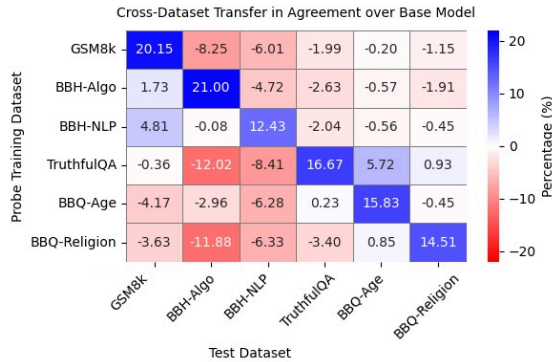


Figure 5. Cross-dataset transfer results measured by agreement improvement over the base model on Llama 3.1 8B Instruct. Rows indicate the dataset used to train the probe, and columns indicate the dataset used for evaluation.

Table 4. Generation accuracy of Qwen2.5 7B Instruct after applying KAPPA to free-form settings.

Method	TruthfulQA	BBQ-Age	GSM8k
Base	41.7	89.7	91.6
KAPPA (1)	44.2	89.9	90.7

Age results in a 5.72% point gain. We further find that differences in the number of options (k) are not a primary barrier to transfer, as evidenced by effective transfer from TruthfulQA ($k = 4$) to BBQ-Age and BBQ-Religion ($k = 3$).

Our analyses on the BBH benchmark further suggest that subspace transfer is more effective between tasks that share similar underlying reasoning skills. Figure 6 shows the distribution of BBH subtasks in which test instances change from incorrect to correct after transfer, for subspaces extracted from different reasoning benchmarks. Here, BBH-Algorithmic mainly comprises subtasks requiring logical reasoning, whereas BBH-NLP emphasizes linguistic and commonsense understanding. When subspaces extracted from GSM8K or BBH-Algorithmic are applied to BBH-NLP, performance gains concentrate on subtasks that involve logical reasoning (e.g., *reasoning about colored objects*, *date understanding*) rather than on linguistic or commonsense tasks (e.g., *movie recommendation*, *ruin names*).

5.2. Applying KAPPA to Free-Form Generation

Setup We evaluate whether KAPPA generalizes beyond MCQs to free-form generation. Specifically, we prompt the model with questions only—without MCQ options—and apply KAPPA at every token generation step, using subspaces extracted from the same dataset under the MCQ setting. For evaluation, we adopt an LLM-as-judge following Chandak et al. (2025), using GPT-4o-mini to compute accuracy.

Results As shown in Table 4, applying KAPPA improves the model accuracy from 41.7% to 44.2%, indicating that

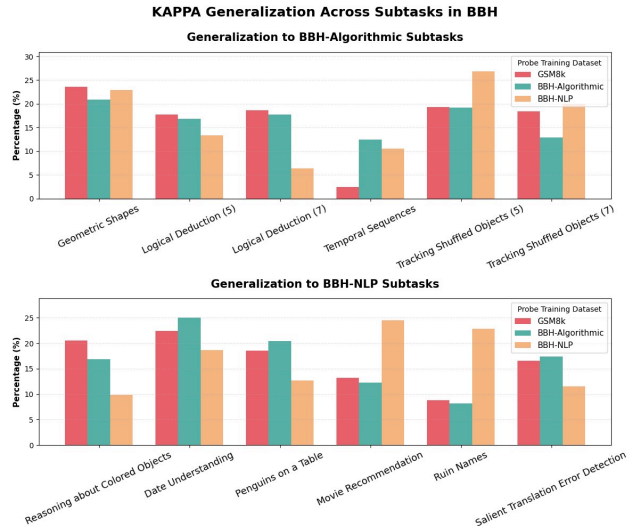


Figure 6. We present a per-subtask analysis of KAPPA generalization on BBH benchmarks. For each probe training dataset (GSM8k, BBH-Algorithmic, BBH-NLP), we identify questions that were originally answered incorrectly by the base model but become correct after applying KAPPA, and report the distribution of these improved questions across BBH subtasks.

KAPPA can generalize to free-form generation. On BBQ-Age, where the base model already exhibits high performance, KAPPA maintains comparable accuracy (89.7% \rightarrow 89.9%). On GSM8K, we observe a slight decrease (91.6% \rightarrow 90.7%), suggesting that for reasoning tasks where the base model is already well optimized for generation settings, the gains from knowledge alignment are limited.

6. Conclusion

This work investigates the knowledge-prediction gap in LLMs and shows that it is pervasive in diverse MCQ settings. Through a geometric analysis of the residual stream, we identify distinct knowledge and prediction subspaces and demonstrate that misalignment between them underlies many model errors. Building on this, we introduce KAPPA, which consistently reduces this gap and improves performance across truthfulness, bias, and reasoning benchmarks at inference time. These results suggest that many failures of LLMs stem not from missing knowledge, but from how the knowledge is utilized. Our findings highlight representation-level alignment as a promising direction for eliciting more faithful model behavior. Several important extensions remain, including developing more reliable methods to extract knowledge from model representations and understanding how nonlinearly encoded knowledge can be aligned.

Impact Statement

This paper presents work whose goal is to advance the understanding of internal representations in large language models and to improve the alignment between model knowledge and predictions. While improved reliability of model outputs may have downstream societal benefits, we do not anticipate significant negative societal impacts specific to this work.

References

- Arditi, A., Obeso, O., Syed, A., Paleka, D., Panickssery, N., Gurnee, W., and Nanda, N. Refusal in language models is mediated by a single direction. In *Proceedings of the 38th International Conference on Neural Information Processing Systems, NIPS '24*, Red Hook, NY, USA, 2024. Curran Associates Inc. ISBN 9798331314385.
- Azaria, A. and Mitchell, T. The internal state of an LLM knows when it’s lying. In Bouamor, H., Pino, J., and Bali, K. (eds.), *Findings of the Association for Computational Linguistics: EMNLP 2023*, pp. 967–976, Singapore, December 2023. Association for Computational Linguistics. doi: 10.18653/v1/2023.findings-emnlp.68. URL <https://aclanthology.org/2023.findings-emnlp.68/>.
- Balepur, N., Rudinger, R., and Boyd-Graber, J. L. Which of these best describes multiple choice evaluation with LLMs? a) forced B) flawed C) fixable D) all of the above. In Che, W., Nabende, J., Shutova, E., and Pilehvar, M. T. (eds.), *Proceedings of the 63rd Annual Meeting of the Association for Computational Linguistics (Volume 1: Long Papers)*, pp. 3394–3418, Vienna, Austria, July 2025. Association for Computational Linguistics. ISBN 979-8-89176-251-0. doi: 10.18653/v1/2025.acl-long.169. URL <https://aclanthology.org/2025.acl-long.169/>.
- Bang, Y. A multitask, multilingual, multimodal evaluation of chatgpt on reasoning, hallucination, and interactivity. *arXiv preprint arXiv:2302.04023*, 2023.
- Brown, T., Mann, B., Ryder, N., Subbiah, M., Kaplan, J. D., Dhariwal, P., Neelakantan, A., Shyam, P., Sastry, G., Askell, A., et al. Language models are few-shot learners. *Advances in neural information processing systems*, 33: 1877–1901, 2020.
- Chandak, N., Goel, S., Prabhu, A., Hardt, M., and Geiping, J. Answer matching outperforms multiple choice for language model evaluation. *arXiv preprint arXiv:2507.02856*, 2025.
- Chuang, Y.-S., Xie, Y., Luo, H., Kim, Y., Glass, J. R., and He, P. Dola: Decoding by contrasting layers improves factuality in large language models. In *The Twelfth International Conference on Learning Representations*, 2024. URL <https://openreview.net/forum?id=Th6NyL07na>.
- Clark, P., Cowhey, I., Etzioni, O., Khot, T., Sabharwal, A., Schoenick, C., and Tafjord, O. Think you have solved question answering? try arc, the ai2 reasoning challenge. *arXiv:1803.05457v1*, 2018.
- Cobbe, K., Kosaraju, V., Bavarian, M., Chen, M., Jun, H., Kaiser, L., Plappert, M., Tworek, J., Hilton, J., Nakano, R., Hesse, C., and Schulman, J. Training verifiers to solve math word problems, 2021. URL <https://arxiv.org/abs/2110.14168>.
- Dziri, N., Lu, X., Sclar, M., Li, X. L., Jiang, L., Lin, B. Y., West, P., Bhagavatula, C., Le Bras, R., Hwang, J. D., Sanyal, S., Welleck, S., Ren, X., Ettinger, A., Harchaoui, Z., and Choi, Y. Faith and fate: limits of transformers on compositionality. In *Proceedings of the 37th International Conference on Neural Information Processing Systems, NIPS '23*, Red Hook, NY, USA, 2023. Curran Associates Inc.
- Gekhman, Z., Ben-David, E., Orgad, H., Ofek, E., Belinkov, Y., Szpektor, I., Herzig, J., and Reichart, R. Inside-out: Hidden factual knowledge in LLMs. In *Second Conference on Language Modeling*, 2025. URL <https://openreview.net/forum?id=f7GG1MbsSM>.
- Góral, G., Wiśnios, E., Sankowski, P., and Budzianowski, P. Wait, that’s not an option: LLMs robustness with incorrect multiple-choice options. In Che, W., Nabende, J., Shutova, E., and Pilehvar, M. T. (eds.), *Proceedings of the 63rd Annual Meeting of the Association for Computational Linguistics (Volume 1: Long Papers)*, pp. 1495–1515, Vienna, Austria, July 2025. Association for Computational Linguistics. ISBN 979-8-89176-251-0. doi: 10.18653/v1/2025.acl-long.75. URL <https://aclanthology.org/2025.acl-long.75/>.
- Gottesman, D. and Geva, M. Estimating knowledge in large language models without generating a single token. In Al-Onaizan, Y., Bansal, M., and Chen, Y.-N. (eds.), *Proceedings of the 2024 Conference on Empirical Methods in Natural Language Processing*, pp. 3994–4019, Miami, Florida, USA, November 2024. Association for Computational Linguistics. doi: 10.18653/v1/2024.emnlp-main.232. URL <https://aclanthology.org/2024.emnlp-main.232/>.
- Hendel, R., Geva, M., and Globerson, A. In-context learning creates task vectors, 2023. URL <https://arxiv.org/abs/2310.15916>.

- Hendrycks, D., Burns, C., Basart, S., Zou, A., Mazeika, M., Song, D., and Steinhardt, J. Measuring massive multitask language understanding. In *International Conference on Learning Representations*, 2021. URL <https://openreview.net/forum?id=d7KBjmI3GmQ>.
- Iharco, G., Ribeiro, M. T., Wortsman, M., Gururangan, S., Schmidt, L., Hajishirzi, H., and Farhadi, A. Editing models with task arithmetic, 2023. URL <https://arxiv.org/abs/2212.04089>.
- Ji, Z., Lee, N., Frieske, R., Yu, T., Su, D., Xu, Y., Ishii, E., Bang, Y. J., Madotto, A., and Fung, P. Survey of hallucination in natural language generation. *ACM computing surveys*, 55(12):1–38, 2023.
- Jin, Q., Dhingra, B., Liu, Z., Cohen, W., and Lu, X. PubMedQA: A dataset for biomedical research question answering. In Inui, K., Jiang, J., Ng, V., and Wan, X. (eds.), *Proceedings of the 2019 Conference on Empirical Methods in Natural Language Processing and the 9th International Joint Conference on Natural Language Processing (EMNLP-IJCNLP)*, pp. 2567–2577, Hong Kong, China, November 2019. Association for Computational Linguistics. doi: 10.18653/v1/D19-1259. URL <https://aclanthology.org/D19-1259/>.
- Kojima, T., Gu, S. S., Reid, M., Matsuo, Y., and Iwasawa, Y. Large language models are zero-shot reasoners. In *Proceedings of the 36th International Conference on Neural Information Processing Systems, NIPS '22*, Red Hook, NY, USA, 2022. Curran Associates Inc. ISBN 9781713871088.
- Lee, B. W., Padhi, I., Ramamurthy, K. N., Miehl, E., Dognin, P., Nagireddy, M., and Dhurandhar, A. Programming refusal with conditional activation steering. In *The Thirteenth International Conference on Learning Representations*, 2025. URL <https://openreview.net/forum?id=Oi47wc10sm>.
- Li, K., Patel, O., Viégas, F., Pfister, H., and Wattenberg, M. Inference-time intervention: Eliciting truthful answers from a language model. In *Thirty-seventh Conference on Neural Information Processing Systems*, 2023. URL <https://openreview.net/forum?id=aLLuYpn83y>.
- Liu, K., Casper, S., Hadfield-Menell, D., and Andreas, J. Cognitive dissonance: Why do language model outputs disagree with internal representations of truthfulness? In Bouamor, H., Pino, J., and Bali, K. (eds.), *Proceedings of the 2023 Conference on Empirical Methods in Natural Language Processing*, pp. 4791–4797, Singapore, December 2023a. Association for Computational Linguistics. doi: 10.18653/v1/2023.emnlp-main-291. URL <https://aclanthology.org/2023.emnlp-main.291/>.
- Liu, S., Ye, H., Xing, L., and Zou, J. In-context vectors: Making in context learning more effective and controllable through latent space steering. *arXiv preprint arXiv:2311.06668*, 2023b.
- Ma, W., He, J., Snell, C., Griggs, T., Min, S., and Zaharia, M. Reasoning models can be effective without thinking. *arXiv preprint arXiv:2504.09858*, 2025.
- Mahaut, M., Aina, L., Czarnowska, P., Hardalov, M., Müller, T., and Marquez, L. Factual confidence of LLMs: on reliability and robustness of current estimators. In Ku, L.-W., Martins, A., and Srikumar, V. (eds.), *Proceedings of the 62nd Annual Meeting of the Association for Computational Linguistics (Volume 1: Long Papers)*, pp. 4554–4570, Bangkok, Thailand, August 2024. Association for Computational Linguistics. doi: 10.18653/v1/2024.acl-long.250. URL <https://aclanthology.org/2024.acl-long.250/>.
- Marks, S. and Tegmark, M. The geometry of truth: Emergent linear structure in large language model representations of true/false datasets, 2024. URL <https://arxiv.org/abs/2310.06824>.
- Orgad, H., Toker, M., Gekhman, Z., Reichart, R., Szpektor, I., Kotek, H., and Belinkov, Y. LLMs know more than they show: On the intrinsic representation of LLM hallucinations. In *The Thirteenth International Conference on Learning Representations*, 2025. URL <https://openreview.net/forum?id=KRnsX5Em3W>.
- Parrish, A., Chen, A., Nangia, N., Padmakumar, V., Phang, J., Thompson, J., Htut, P. M., and Bowman, S. BBQ: A hand-built bias benchmark for question answering. In Muresan, S., Nakov, P., and Villavicencio, A. (eds.), *Findings of the Association for Computational Linguistics: ACL 2022*, pp. 2086–2105, Dublin, Ireland, May 2022. Association for Computational Linguistics. doi: 10.18653/v1/2022.findings-acl.165. URL <https://aclanthology.org/2022.findings-acl.165/>.
- Pezeshkpour, P. and Hruschka, E. Large language models sensitivity to the order of options in multiple-choice questions. In Duh, K., Gomez, H., and Bethard, S. (eds.), *Findings of the Association for Computational Linguistics: NAACL 2024*, pp. 2006–2017, Mexico City, Mexico, June 2024. Association for Computational Linguistics. doi: 10.18653/v1/2024.findings-naacl.130. URL <https://aclanthology.org/2024.findings-naacl.130/>.

- Rimsky, N., Gabrieli, N., Schulz, J., Tong, M., Hubinger, E., and Turner, A. Steering llama 2 via contrastive activation addition. In Ku, L.-W., Martins, A., and Srikumar, V. (eds.), *Proceedings of the 62nd Annual Meeting of the Association for Computational Linguistics (Volume 1: Long Papers)*, pp. 15504–15522, Bangkok, Thailand, August 2024. Association for Computational Linguistics. doi: 10.18653/v1/2024.acl-long.828. URL <https://aclanthology.org/2024.acl-long.828/>.
- Shen, T., Li, J., Bouadjenek, M. R., Mai, Z., and Sanner, S. Towards understanding and mitigating unintended biases in language model-driven conversational recommendation. *Inf. Process. Manage.*, 60(1), January 2023. ISSN 0306-4573. doi: 10.1016/j.ipm.2022.103139. URL <https://doi.org/10.1016/j.ipm.2022.103139>.
- Su, W., Wang, C., Ai, Q., Hu, Y., Wu, Z., Zhou, Y., and Liu, Y. Unsupervised real-time hallucination detection based on the internal states of large language models. In Ku, L.-W., Martins, A., and Srikumar, V. (eds.), *Findings of the Association for Computational Linguistics: ACL 2024*, pp. 14379–14391, Bangkok, Thailand, August 2024. Association for Computational Linguistics. doi: 10.18653/v1/2024.findings-acl.854. URL <https://aclanthology.org/2024.findings-acl.854/>.
- Sun, Y., Stolfo, A., and Sachan, M. Probing for arithmetic errors in language models. In Christodoulopoulos, C., Chakraborty, T., Rose, C., and Peng, V. (eds.), *Proceedings of the 2025 Conference on Empirical Methods in Natural Language Processing*, pp. 8111–8128, Suzhou, China, November 2025a. Association for Computational Linguistics. ISBN 979-8-89176-332-6. doi: 10.18653/v1/2025.emnlp-main.411. URL <https://aclanthology.org/2025.emnlp-main.411/>.
- Sun, Y., Wang, H., Li, J., Liu, J., Li, X., Wen, H., Yuan, Y., Zheng, H., Liang, Y., Li, Y., and Liu, Y. An empirical study of LLM reasoning ability under strict output length constraint. In Christodoulopoulos, C., Chakraborty, T., Rose, C., and Peng, V. (eds.), *Proceedings of the 2025 Conference on Empirical Methods in Natural Language Processing*, pp. 7652–7671, Suzhou, China, November 2025b. Association for Computational Linguistics. ISBN 979-8-89176-332-6. doi: 10.18653/v1/2025.emnlp-main.389. URL <https://aclanthology.org/2025.emnlp-main.389/>.
- Suzgun, M., Scales, N., Schärli, N., Gehrmann, S., Tay, Y., Chung, H. W., Chowdhery, A., Le, Q., Chi, E., Zhou, D., and Wei, J. Challenging BIG-bench tasks and whether chain-of-thought can solve them. In Rogers, A., Boyd-Graber, J., and Okazaki, N. (eds.), *Findings of the Association for Computational Linguistics: ACL 2023*, pp. 13003–13051, Toronto, Canada, July 2023. Association for Computational Linguistics. doi: 10.18653/v1/2023.findings-acl.824. URL <https://aclanthology.org/2023.findings-acl.824/>.
- Tulchinskii, E., Kushnareva, L., Kuznetsov, K., Voznyuk, A., Andriianen, A., Piontkovskaya, I., Burnaev, E., and Barannikov, S. Listening to the wise few: Select-and-copy attention heads for multiple-choice qa, 2024. URL <https://arxiv.org/abs/2410.02343>.
- Turner, A. M., Thiergart, L., Leech, G., Udell, D., Vazquez, J. J., Mini, U., and MacDiarmid, M. Steering language models with activation engineering. *arXiv preprint arXiv:2308.10248*, 2023.
- Venhoff, C., Arcuschin, I., Torr, P., Conmy, A., and Nanda, N. Understanding reasoning in thinking language models via steering vectors. In *Workshop on Reasoning and Planning for Large Language Models*, 2025. URL <https://openreview.net/forum?id=OwhVWNOBcz>.
- von Rütte, D., Anagnostidis, S., Bachmann, G., and Hofmann, T. A language model’s guide through latent space. In *Proceedings of the 41st International Conference on Machine Learning, ICML’24*. JMLR.org, 2024.
- Wang, Y., Li, H., Zou, H., Zhang, J., He, X., Li, Q., and Xu, K. Hidden question representations tell non-factuality within and across large language models. *CoRR*, abs/2406.05328, 2024. URL <https://doi.org/10.48550/arXiv.2406.05328>.
- Wei, J., Wang, X., Schuurmans, D., Bosma, M., brian ichter, Xia, F., Chi, E. H., Le, Q. V., and Zhou, D. Chain of thought prompting elicits reasoning in large language models. In Oh, A. H., Agarwal, A., Belgrave, D., and Cho, K. (eds.), *Advances in Neural Information Processing Systems*, 2022. URL https://openreview.net/forum?id=_VjQlMeSB_J.
- Wen, B., Howe, B., and Wang, L. L. Characterizing LLM abstention behavior in science QA with context perturbations. In Al-Onaizan, Y., Bansal, M., and Chen, Y.-N. (eds.), *Findings of the Association for Computational Linguistics: EMNLP 2024*, pp. 3437–3450, Miami, Florida, USA, November 2024. Association for Computational Linguistics. doi: 10.18653/v1/2024.findings-emnlp.197. URL <https://aclanthology.org/2024.findings-emnlp.197/>.
- Wiegrefe, S., Taffjord, O., Belinkov, Y., Hajishirzi, H., and Sabharwal, A. Answer, assemble, ace: Understanding

how LMs answer multiple choice questions. In *The Thirteenth International Conference on Learning Representations*, 2025. URL <https://openreview.net/forum?id=6NNA0MxhCH>.

Yang, Y., Chern, E., Qiu, X., Neubig, G., and Liu, P. Alignment for honesty. In *The Thirty-eighth Annual Conference on Neural Information Processing Systems*, 2024. URL <https://openreview.net/forum?id=67K3X1vw8L>.

Yang, Z., Jian, P., and Li, C. Option symbol matters: Investigating and mitigating multiple-choice option symbol bias of large language models. In Chiruzzo, L., Ritter, A., and Wang, L. (eds.), *Proceedings of the 2025 Conference of the Nations of the Americas Chapter of the Association for Computational Linguistics: Human Language Technologies (Volume 1: Long Papers)*, pp. 1902–1917, Albuquerque, New Mexico, April 2025. Association for Computational Linguistics. ISBN 979-8-89176-189-6. doi: 10.18653/v1/2025.naacl-long.95. URL <https://aclanthology.org/2025.naacl-long.95/>.

Zheng, C., Zhou, H., Meng, F., Zhou, J., and Huang, M. Large language models are not robust multiple choice selectors. In *The Twelfth International Conference on Learning Representations*, 2024. URL <https://openreview.net/forum?id=shr9PXz7T0>.

Zou, A., Phan, L., Chen, S., Campbell, J., Guo, P., Ren, R., Pan, A., Yin, X., Mazeika, M., Dombrowski, A.-K., et al. Representation engineering: A top-down approach to ai transparency. *arXiv preprint arXiv:2310.01405*, 2023.

Zou, A., Phan, L., Chen, S., Campbell, J., Guo, P., Ren, R., Pan, A., Yin, X., Mazeika, M., Dombrowski, A.-K., Goel, S., Li, N., Byun, M. J., Wang, Z., Mallen, A., Basart, S., Koyejo, S., Song, D., Fredrikson, M., Kolter, J. Z., and Hendrycks, D. Representation engineering: A top-down approach to ai transparency, 2025. URL <https://arxiv.org/abs/2310.01405>.

A. Data Statistics

To adapt BBH and TruthfulQA to our experimental framework, we standardize all items to four-choice multiple-choice questions. For items originally containing more than four options, we randomly sample three incorrect options and combine them with the correct answer. This procedure ensures a consistent MCQ format while preserving the original label distribution. For BBH and MMLU, we construct evaluation sets based on the subtask compositions defined in the original benchmark papers. In the case of BBH, we exclude subtasks that contain only two or three options or cannot be naturally formatted as MCQs, retaining only those with four or more options that support unambiguous multiple-choice formatting. The complete list of included subtasks for BBH and MMLU is provided in Table 5 and Table 6, respectively.

Table 7 summarizes the number of samples in each split and the number of answer choices for each dataset. Each question is evaluated under multiple option orders. This procedure neutralizes positional biases while preserving exact class balance across the entire dataset.

Table 5. Subtasks used from the BBH-Algorithmic and BBH-NLP benchmarks.

Dataset	BBH-Algorithmic	BBH-NLP
Subtasks	geometric shapes	date understanding
	logical deduction	penguins in a table
	temporal sequences	movie recommendation
	tracking shuffled objects	ruin names
	reasoning about colored objects	salient translation error detection

Table 6. Subtasks used from the MMLU Humanities, Social Sciences, and STEM benchmarks.

Dataset	Subtasks	
MMLU Humanities	Formal Logic	Moral Disputes
	High School European History	Moral Scenarios
	High School US History	Philosophy
	High School World History	Prehistory
	International Law	Professional Law
	Jurisprudence	World Religions
	Logical Fallacies	
MMLU Social Sciences	High School Geography	Professional Psychology
	High School Gov't and Politics	Public Relations
	High School Macroeconomics	Security Studies
	High School Microeconomics	Sociology
	High School Psychology	US Foreign Policy
	Human Sexuality	
MMLU STEM	Abstract Algebra	Electrical Engineering
	Anatomy	Elementary Mathematics
	Astronomy	High School Biology
	College Biology	High School Chemistry
	College Chemistry	High School Computer Science
	College Computer Science	High School Mathematics
	College Mathematics	High School Physics
	College Physics	High School Statistics
	Computer Security	Machine Learning

B. Optimized Transformation of KAPPA

B.1. Derivation of the Closed-form Update

We rewrite our optimization problem Eq. 3 as:

$$\min_{h'} \|h' - h\|_2^2 \quad \text{s.t.} \quad W_{\text{pred}}^\top h' + b_{\text{pred}} = W_{\text{know}}^\top h + b_{\text{know}}.$$

Table 7. Dataset statistics for training, validation, and test splits. k denotes the number of answer choices.

Category	Dataset	k	Train	Validation	Test
Reasoning	GSM8k	4	8960	2992	10552
	BBH-Algorithmic	4	4800	2400	4800
	BBH-NLP	4	4464	2232	4472
Knowledge	MMLU Humanities	4	15000	7536	15104
	MMLU Social Sciences	4	9800	4936	9880
	MMLU STEM	4	10040	5064	10120
	ARC-Challenge	3	6714	1794	7032
	PubMedQA	3	2400	600	3000
Truthfulness & Bias	TruthfulQA	4	2208	1104	2208
	BBQ-Age	3	8832	4416	8832
	BBQ-Religion	3	2880	1440	2880

First, we define the target prediction coordinates

$$p_{\text{target}} := W_{\text{know}}^{\top} h + b_{\text{know}} - b_{\text{pred}} \in \mathbb{R}^k,$$

so the constraint becomes

$$W_{\text{pred}}^{\top} h' = p_{\text{target}}.$$

Then we form the Lagrangian

$$\mathcal{L}(h', \lambda) = \|h' - h\|_2^2 + \lambda^{\top} (W_{\text{pred}}^{\top} h' - p_{\text{target}}), \quad \lambda \in \mathbb{R}^k.$$

Setting the gradient with respect to h' to zero gives

$$2(h' - h) + W_{\text{pred}} \lambda = 0 \implies h' = h - \frac{1}{2} W_{\text{pred}} \lambda.$$

Substituting into the constraint yields

$$W_{\text{pred}}^{\top} (h - \frac{1}{2} W_{\text{pred}} \lambda) = p_{\text{target}},$$

which is equivalent to

$$W_{\text{pred}}^{\top} W_{\text{pred}} \lambda = 2 (W_{\text{pred}}^{\top} h - p_{\text{target}}).$$

Let

$$G := W_{\text{pred}}^{\top} W_{\text{pred}} \in \mathbb{R}^{k \times k}$$

denote the Gram matrix. When the columns of W_{pred} are linearly independent, G is invertible and

$$\lambda = 2G^{-1} (W_{\text{pred}}^{\top} h - p_{\text{target}}).$$

Plugging this into the expression for h' gives the closed-form update

$$h' = h + W_{\text{pred}} G^{-1} (p_{\text{target}} - W_{\text{pred}}^{\top} h).$$

B.2. Interpretations of the Closed-form Update

The solution yields the closed-form update, which is an affine transformation of h :

$$h' = \left(I - \frac{W_{\text{pred}} W_{\text{pred}}^{\top}}{\|W_{\text{pred}}\|^2} \right) h + \frac{p_{\text{target}}}{\|W_{\text{pred}}\|^2} W_{\text{pred}}.$$

Note that the original hidden state h can be decomposed as

$$h = \left(I - \frac{W_{\text{pred}} W_{\text{pred}}^{\top}}{\|W_{\text{pred}}\|^2} \right) h + \frac{W_{\text{pred}}^{\top} h}{\|W_{\text{pred}}\|^2} W_{\text{pred}}.$$

Compared to this decomposition, our update h' simply replaces the prediction coordinate $\frac{W_{\text{pred}}^{\top} h}{\|W_{\text{pred}}\|^2}$ with $\frac{p_{\text{target}}}{\|W_{\text{pred}}\|^2}$, while leaving all orthogonal components unchanged.

C. Experimental Setup Details

C.1. Prompt Formats

To mitigate the effects of option bias—where the model favors a particular choice (Zheng et al., 2024; Pezeshkpour & Hruschka, 2024)—we evaluate the base model across multiple prompt formats (32 combinations), derived from four alternative instructions, two answer formats, and four option symbols, and select the format that yields the most balanced predictions on the validation set. We present each component in Table 8, Table 9, and Table 10.

Table 8. Task instructions used in our experiments.

Instruction	Text
1	Provide your answer with {option_text}, following the output format below. Output Format: {format_text}
2	Given the following question and candidate answers, choose the correct option. Output Format: {format_text}
3	Choose the correct option between {option_text}. Use the format shown below when you answer. Output Format: {format_text}
4	Choose the best answer. Follow the output format below. Output Format: {format_text}

Table 9. Answer format types used in experiments.

Answer Format Type	Format Text
1	The correct answer is (
2	Answer: (

Table 10. Option symbol types used in experiments.

Option Symbol Type	Examples
Common Alphabet Upper	(A), (B), (C), (D)
Roman Numerals	(i), (ii), (iii), (iv)
Common Numbers	(1), (2), (3), (4)
Random Alphabet Upper	(Q), (K), (E), (U)

C.2. Prompt Example

We present one example of the prompt format used in our experiments, shown below.

Multiple-Choice Prompt

Instruction. Choose the correct option between (1), (2), (3), or (4). Use the format shown below when you answer.

Output Format.

The correct answer is (1) or

The correct answer is (2) or

The correct answer is (3) or

The correct answer is (4)

Question.

In Python 3, which of the following functions converts a string to an integer?

Choices.

(1) `float(x)`

(2) `int(x[, base])`

(3) `long(x[, base])`

(4) `str(x)`

C.3. KAPPA Evaluation Protocol

Our evaluation of KAPPA proceeds in three stages. First, we evaluate all prompt formats on the validation set and select the format yielding the most balanced predictions across answer options. This enables us to isolate the knowledge-prediction gap from the positional bias in multiple-choice questions. Second, we extract activations from all model layers and train both the knowledge probe and the prediction probe. For probe training, we use a batch size of 128, learning rate of 0.0002, and select the checkpoint with the best validation accuracy across 1000 epochs. We select layers whose prediction probe accuracy exceeds 85% on the validation set, and then identify the top n consecutive layers based on knowledge probe performance on the same validation set. Finally, we apply 1-layer, 3-layer, and 6-layer KAPPA to the test datasets. Without model- or dataset-specific hyperparameter tuning, we use consistent settings across all configurations: $\alpha = 30, \beta = 0$ for single-layer interventions and $\alpha = 10, \beta = 0$ for multi-layer interventions.

C.4. Baselines

Base The original large language model (LLM) without any intervention or modification. This baseline reflects the model’s raw performance on the evaluation datasets.

Contrastive Activation Addition (CAA) Following [Rimsky et al. \(2024\)](#), for each training example, we construct two prompted sequences in the same format, “user {instruction}{question}{option} assistant The answer is (X)”, one with the correct option $X = y$ and one with a randomly sampled incorrect option $X \neq y$. We then run the LLM on these sequences and extract the residual stream activation at the final token position from every layer. Let h_{corr}^l and h_{incorr}^l denote the resulting activations at layer l for the correct and incorrect sequences, respectively. We define a steering vector at each layer as the mean difference $v^{(l)} = \mathbb{E}[h_{\text{corr}}^l - h_{\text{incorr}}^l]$.

To select the intervention layer, we apply each candidate vector $v^{(l)}$ once on the validation set by adding it to the residual stream at layer l , and choose the single layer that maximizes validation accuracy. We then evaluate on the test set using the selected layer, with a fixed multiplier of 1.0 for the intervention, following [Rimsky et al. \(2024\)](#).

Decoding by Contrasting Layers (DoLA) We evaluate the dynamic variant of DoLA following [Chuang et al. \(2024\)](#). Specifically, we select the optimal layer bucket by evaluating all candidate buckets on the validation set, and then apply the selected bucket for evaluation on the test set. Since our setting focuses on single-token prediction, we set the hyperparameter $\alpha = 0$ throughout the experiments.

D. Additional Results

D.1. Linear Probing Results

Figure 7 presents probing results across benchmarks using Llama 3.1 8B Instruct, showing that the probe trained to predict correct answers achieves stable performance across layers, consistently exceeding the base model accuracy.

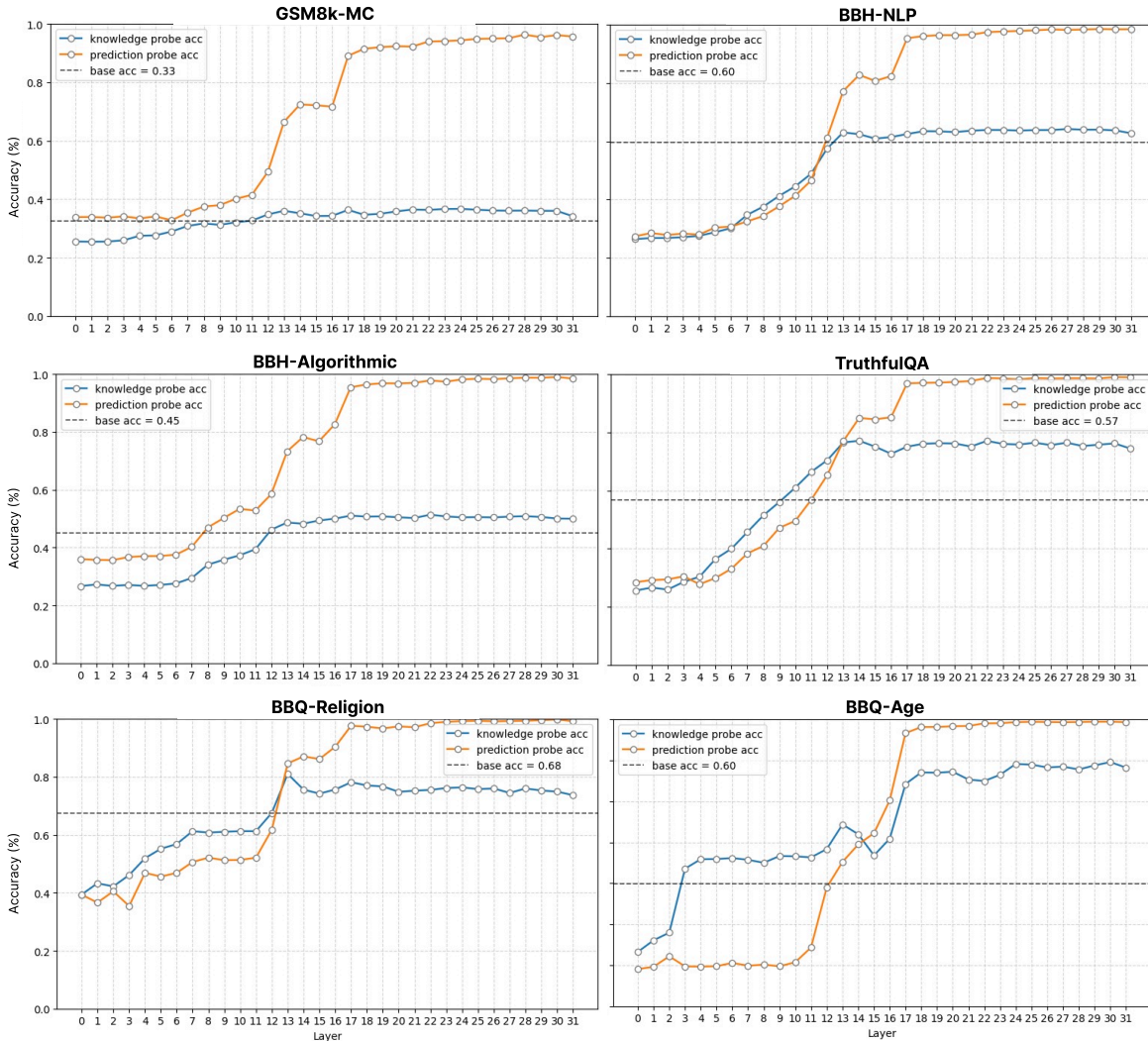


Figure 7. Layer-wise accuracy of knowledge probes (blue) and prediction probes (orange) across benchmarks, with baseline accuracy shown as dashed lines. Prediction probe accuracy reaches very high levels in later layers, and knowledge probe accuracy consistently exceeds baseline model accuracy, suggesting a significant knowledge-prediction gap.

D.2. KAPPA Intervention Results

Results Across Datasets Table 11 reports results on knowledge-oriented benchmarks for Qwen 2.5 7B Instruct and Llama 3.1 8B Instruct. Across these datasets, where the knowledge-prediction gap is relatively smaller than in reasoning or bias benchmarks, we still observe that KAPPA consistently improves agreement (AGR), indicating more faithful alignment between linearly accessible knowledge and model predictions. At the same time, gains in task accuracy (ACC) remain modest. This is expected, as the performance of the knowledge probe itself is comparatively low on these benchmarks, limiting the potential upper bound for accuracy improvements. Nevertheless, KAPPA yields non-trivial accuracy gains in some settings, suggesting that even when the gap is less pronounced, improving representation-level alignment can still translate into more reliable predictions.

Bridging the Knowledge-Prediction Gap in LLMs on Multiple-Choice Questions

Table 11. Results across knowledge benchmarks for Qwen 2.5 7B Instruct and Llama 3.1 8B Instruct. Higher Δ ACC and AGR indicate smaller knowledge-prediction gaps, while lower KLD reflects closer alignment between encoded knowledge and model predictions. Benchmark names annotated with (\cdot) denote the number of answer options in the corresponding MCQ setting. The KP rows report results computed directly from the knowledge probe’s predictions. For KAPPA(\cdot), the value in parentheses denotes the number of layers intervened at inference time. Boldface indicates the best result among {Base, CAA, DoLA, KAPPA(\cdot)}, excluding the KP row.

Model	Method	MMLU Humanities			MMLU Social Sciences			MMLU STEM			PubMedQA		
		ACC	AGR	KLD	ACC	AGR	KLD	ACC	AGR	KLD	ACC	AGR	KLD
Qwen 2.5 7B	Base	59.91	78.50	0.777	78.85	95.93	0.718	65.17	89.70	0.703	72.33	89.80	0.570
	CAA	59.92	78.42	0.777	78.81	95.94	0.718	65.19	89.50	0.708	72.27	89.63	0.570
	DoLA	59.85	78.64	0.811	78.52	94.81	0.725	65.60	87.81	0.714	71.63	89.63	0.570
	KAPPA (1)	60.77	82.03	0.751	78.91	97.12	0.734	65.24	93.17	0.721	72.57	91.43	0.565
	KAPPA (3)	61.04	82.23	0.720	78.95	96.78	0.739	65.45	92.70	0.724	72.53	91.37	0.565
	KAPPA (6)	61.92	85.22	0.703	79.12	95.47	0.759	65.56	91.99	0.764	73.00	90.70	0.588
	KP	62.47	100.00	0.000	79.02	100.00	0.000	65.36	100.00	0.000	72.00	100.00	0.000
Llama 3.1 8B	Base	58.57	77.94	0.469	74.04	90.55	0.471	54.65	91.12	0.321	75.73	96.43	0.434
	CAA	59.62	77.56	0.487	73.93	90.62	0.466	54.85	90.09	0.344	75.10	94.37	0.467
	DoLA	56.08	69.35	0.504	72.25	84.00	0.571	51.76	71.36	0.533	74.63	92.53	0.536
	KAPPA (1)	60.67	87.15	0.533	73.79	96.08	0.617	54.34	90.56	0.684	75.17	96.77	0.576
	KAPPA (3)	60.32	85.19	0.456	73.24	94.54	0.607	54.03	86.30	0.755	75.33	98.57	0.566
	KAPPA (6)	60.73	87.00	0.446	70.49	85.98	0.778	54.23	84.58	0.899	76.03	96.97	0.599

Table 12. Average accuracy (ACC), agreement (AGR), and KL divergence (KLD) across multiple models on the GSM8k benchmark. For KAPPA(\cdot), the value in parentheses denotes the number of layers intervened at inference time. Boldface indicates the best result among {Base, CAA, DoLA, KAPPA(\cdot)}, excluding the knowledge probe (KP).

Method	GSM8k														
	Mistral v0.3 7B			Llama-3.1 8B			Qwen 2.5 7B			Qwen3 4B			Qwen3 14B		
	ACC	AGR	KLD	ACC	AGR	KLD	ACC	AGR	KLD	ACC	AGR	KLD	ACC	AGR	KLD
Base	31.7	58.3	0.41	32.6	53.7	0.35	47.8	60.3	0.86	47.1	70.4	0.57	63.5	63.5	0.74
CAA	31.8	58.4	0.42	32.9	53.8	0.38	47.7	60.3	0.85	47.1	70.5	0.62	64.3	63.1	0.76
DoLA	31.7	55.7	0.62	33.2	49.7	0.58	48.1	60.0	0.86	46.0	66.1	0.67	62.6	60.7	0.77
KAPPA (1)	33.0	79.0	0.54	34.9	73.8	0.37	49.6	68.8	0.78	47.5	76.2	0.56	53.0	73.8	0.74
KAPPA (3)	33.6	83.8	0.48	34.6	66.2	0.27	49.1	65.4	0.77	47.2	72.8	0.71	61.3	72.7	0.72
KAPPA (6)	33.6	72.5	0.49	36.6	75.9	0.27	49.2	66.3	0.76	46.7	73.2	0.70	60.8	69.0	0.79
KP	34.0	100.0	0.00	36.6	100.0	0.00	50.3	100.0	0.00	46.7	100.0	0.00	56.6	100.0	0.00

Results Across Models Table 12 reports the average accuracy (ACC), agreement rate (AGR), and KL divergence (KLD) across multiple models on the GSM8k benchmark. Across all model families, KAPPA consistently increases AGR relative to the base model, demonstrating its effectiveness in mitigating the knowledge-prediction gap. This suggests that KAPPA reliably encourages models to better utilize their linearly accessible knowledge during inference, even on challenging mathematical reasoning tasks.